Applied Clay Science 99 (2014) 72–82

Contents lists available at ScienceDirect

Applied Clay Science

journal homepage: www.elsevier.com/locate/clay

Research paper

Synthesis and characterization of organosaponites. Thermal behavior of their poly(vinyl chloride) nanocomposites

S. Albeniz [a], M.A. Vicente [b], R. Trujillano [b], S.A. Korili [a], A. Gil [a,*]

[a] Department of Applied Chemistry, Building Los Acebos, Public University of Navarra, Campus of Arrosadía, E-31006 Pamplona, Spain
[b] Department of Inorganic Chemistry, Faculty of Chemical Science, Square of Merced, University of Salamanca, E-37008 Salamanca, Spain

ARTICLE INFO

Article history:
Received 21 February 2014
Received in revised form 11 June 2014
Accepted 12 June 2014
Available online 30 June 2014

Keywords:
Saponite
Organoclay
Titanium modified saponite
PVC
Surfactant

ABSTRACT

The aim of this work was to synthesize and characterize the structural properties of the materials resulting from the combination of a synthetic saponite with several organic molecules, namely, Arquad 2HT-75, octadecylamine, 3-aminopropyltriethoxysilane, trimethyloctadecylammonium bromide and tetraethoxysilane, or combinations of them, and with or without the addition of HCl during synthesis. The ratios organic molecule/saponite and HCl/organic molecule were considered as synthesis variables. Structural characterization was based on X-ray diffraction (XRD), simultaneous thermogravimetric/differential thermal analysis (TG/DTA) and infrared spectroscopy (FTIR). The chemical composition of the materials was determined through X-ray fluorescence (XRF) and atomic absorption spectroscopy (AAS), and their morphology was analyzed through scanning electron microscopy (SEM). The values obtained for the basal spacings were a function of the type and amount of the organic molecule. Otherwise, HCl did not significantly influence the basal spacing, but it had the capacity to significantly modify the morphology and the chemical composition of the samples. From the results found, the solids modified with tetraethoxysilane and 3-aminopropyltriethoxysilane were selected to incorporate various titanium precursors. These new organo-modified saponites were used in the formulation of PVC nanocomposites and their thermal behavior was evaluated at two temperatures (70 and 180 °C).

© 2014 Elsevier B.V. All rights reserved.

1. Introduction

The utility of inorganic nanoparticles as additives to enhance polymer performance has been reported in the last years. The clay polymer nanocomposites (CPN) are of particular interest because of their enhancements, relative to an unmodified polymer, in a large number of physical properties including mechanical properties, gas permeability, fire and thermal resistance, environmental stability and solvent uptake (Pinnavaia and Beall, 2000).

Among the large number of inorganic layered materials that exhibit intercalation capabilities, layered silicates form one of the most typical groups because of their reaction versatility. In particular, clay minerals of the smectite group, such as montmorillonite, saponite and hectorite, have mainly been used because they have excellent intercalation abilities. Several reviews have recently appeared on CPN based on smectites (Bergaya et al., 2013; Chen et al., 2008; Galimberti et al., 2013; Giannelis, 1996; Lagaly, 1999; LeBaron et al., 1999; Pavlidou and Papaspyrides, 2008; Sinha Ray and Okamoto, 2003). Studies on layered silicate–polymer compounds based on other types of layered silicates have been conducted to a much lesser degree because of the relative difficulties in the preparation of the polymer-intercalated compounds.

Polymer and smectite are not miscible due to the hydrophilicity of the clay mineral layers and because most of the polymer is hydrophobic. Thus, the compatibility is not enough for the polymer chains to intercalate into the clay interlayer spaces. To solve this problem, inorganic smectites are modified with organic molecules by ion exchange resulting in organoclays (OC) (Lambert and Bergaya, 2013; Moghri and Akbarian, 2009). OC are essential to developed CPN, materials formed by the combination of two or more materials, producing unique and synergic properties, different from those of the individual components (Betega de Paiva et al., 2008).

Poly(vinyl chloride) (PVC) is one of the polymers with the highest production and applications (Dunlap and Desch, 1982) due to its characteristics such as easy modification and low cost. This polymer still has problems with its low thermal stability during manufacture and use. For that, the effect of the incorporation of additives as stabilizers, lubricants, plasticizers, fillers, etc. has been considered as topic in the PVC research. Among these possibilities, the use of layered clay minerals has been described by several investigators as an efficient method to modify and control the thermal stability of PVC (Awad et al., 2009; Gong et al., 2004; Liu et al., 2008; Peprnicek et al., 2006; Wu et al., 2010). The effect of the presence of titanium oxide has also been

* Corresponding author. Tel./fax: +34 948 169602.
E-mail address: andoni@unavarra.es (A. Gil).

http://dx.doi.org/10.1016/j.clay.2014.06.014
0169-1317/© 2014 Elsevier B.V. All rights reserved.

reported to reduce the photodegradation of this polymer (Gesenhues, 2000; Kemp and McIntyre, 2006).

The present study aims to synthesize and characterize the structural properties of materials resulting from the combination of a saponite with several organic molecules, namely Arquad 2HT-75, octadecylamine, 3-aminopropyltriethoxysilane, trimethyloctadecylammonium bromide and tetraethoxysilane, or combinations of them, that can be used as nanofillers of CPN. The OC with best properties will be selected to incorporate various titanium sources. These new organo-modified saponites will be used in the formulation of PVC nanocomposites and the thermal behavior will be evaluated at two temperatures (see Scheme 1).

2. Experimental

2.1. Raw material and preparation of organically modified saponite

The starting material was a synthetic saponite (Sap) from Kunimine, supplied by The Clay Science Society of Japan. The raw clay mineral is very pure, which allows a better identification by instrumental techniques. Its cationic exchange capacity (CEC) is 100 meq/100 g.

The organic molecules employed in this work to modify the clay mineral were: Arquad 2HT-75 (Fluka, H_2O 8–12%), mainly composed of dimethyldioctadecylammonium chloride, although it may also contain C_{16} chains; octadecylamine ($CH_3(CH_2)_{17}NH_2$, Aldrich, 90%); 3-aminopropyltriethoxysilane ($H_2N(CH_2)_3Si(OC_2H_5)_3$, Aldrich, 99%); trimethyloctadecylammonium bromide ($CH_3(CH_2)_{17}N(Br)(CH_3)_3$, Aldrich, 98%) and tetraethoxysilane ($Si(OC_2H_5)_4$, Alfa Aesar, 98%).

The syntheses of the modified Sap were carried out by cation-exchange. All samples were prepared by adding the necessary amount of surfactant to obtain 0.5, 1, 2 and 5 times the CEC of the clay mineral. The samples obtained and their nomenclature are summarized in Table 1.

Two methods were used to prepare the samples. In the first one, 5 g of Sap was stirred with the appropriate amount of surfactant and 250 cm^3 of deionized water in a centrifuge flask for 4 h at 50 °C. The solutions were separated from the solid by centrifugation for 20 min at 4500 rpm and washed three times with deionized water. Finally, the samples were dried for 14 h in air at 120 °C. The second method was only used to prepare the samples organofunctionalized with tetraethoxysilane (TEOS). This process was carried out in two steps: in the first step 5 g of Sap was dispersed in 15 cm^3 of 2-propanol with magnetic stirring, then deionized water and the necessary amount of TEOS was added until a homogeneous white gel was formed. This gel was dried at 60 °C in an oven to obtain S-TEOS. In the second step, 5 g of ground S-TEOS was stirred for 48 h with 3-aminopropyltriethoxysilane and 50 cm^3 of 2-propanol. Finally, the mixture was dried at 60 °C to obtain the final solid.

2.2. Preparation of titanium modified saponite and saponite PVC nanocomposite

A modification of the second method reported previously was used to prepare the samples with titanium. In the first step, 5 g of Sap was dispersed in 15 cm^3 of 2-propanol with magnetic stirring, then deionized water and 4.84 cm^3 of TEOS was added until a homogeneous white gel was formed. This gel was dried at 60 °C in an oven to obtain S-TEOS(5). In the second step, 5 g of ground S-TEOS(5) was stirred for 48 h with 50 cm^3 of 2-propanol, 3.19 cm^3 of 3-aminopropyltriethoxysilane and the titanium sources. The titanium sources were: titanium (IV) bis(ammonium lactate) dihydroxide ($[CH_3CH(O\text{-})CO_2NH_4]_2Ti(OH)_2$, $C_6H_{18}N_2O_8Ti$, Aldrich, 50 mass% in water); titanium (IV)-isopropoxide ($Ti[OCH(CH_3)_2]_4$, $C_{12}H_{28}O_4Ti$, Aldrich, 97%); titanium (IV) ethoxide ($Ti(OC_2H_5)_4$, $C_8H_{20}O_4Ti$, Aldrich) and titanium(IV) oxide (rutile, Aldrich, 99.99%). Finally, the mixtures were dried at 60 °C and calcined at 850 °C for 4 h to obtain the final solids. The samples obtained and their nomenclature are summarized in Table 2. The number of the C atoms of the titanium source was included in the nomenclature.

The formulation of Sap PVC nanocomposite was: 1 g of PVC, 0.8 g of $CaCO_3$, 0.03 g of stabilizing Ca/Zn, 0.8 g of plasticizer di-iso-nonyl phthalate and 0.08 g of titanium OC. All components are mixed with 25 cm^3 of tetrahydrofuran (HPLC purity) ultrasonically agitated for 1 h. After this time, a whitish homogeneous mixture is formed. This mixture is poured into a cylindrical mold, followed by evaporation of the solvent. Finally, plates with 1.5 × 1.5 cm square and 1 mm thick were obtained.

2.3. Characterization techniques

XRD patterns of the materials were obtained using a Siemens D-5000 diffractometer using Cu Kα filtered radiation (λ = 0.1548 nm). The working conditions employed were 30 mA, 40 kV and a scanning rate of 2° (2θ)/min.

Elemental analyses of the solids were carried out by the Instituto Geológico y Minero, Spain, using XRF and AAS, while special analyses were carried out for the determination of C.

Thermal analyses were performed on TA-Instruments, TGA2950. The measurements were carried out at a heating rate of 10 °C/min from room temperature to 800 °C under nitrogen atmosphere.

FT-IR spectra were recorded on a Perkin-Elmer 1730 Infrared Fourier Transform Spectrometer provided with a laser radiation source of He–Ne (λ = 632.8 nm). The spectra were performed using the KBr pellet technique, with a KBr:sample ratio of 300:1. The spectral region studied was between 400 and 4000 cm^{-1}.

SEM and Energy-Dispersive X-ray (EDX) analysis were performed using a Digital Scanning Microscope Zeiss DSM 940, operating at

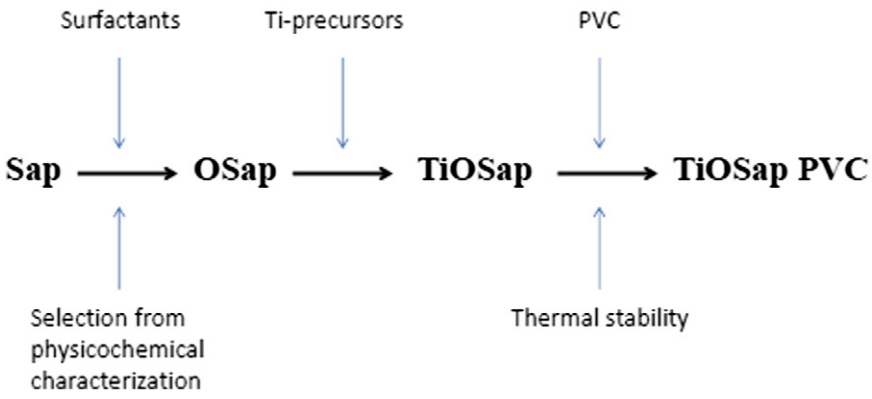

Scheme 1. Synthesis steps of OSap PVC nanocomposites.

Table 1
Nomenclature and preparation conditions of the organically modified saponites synthesized.

Sample[a]	Surfactant	Parameter varied (x = 0.5, 1, 2 and 5 CEC)[a]	Parameter fixed (CEC)	Method of synthesis
Sap-Aq(x)	Arquad 2HT-75	Aq		1st method
Sap-Aq(0.5)–HCl(x)	Arquad 2HT-75/HCl	HCl	Aq(0.5)	1st method
Sap-Oc(0.5)–HCl(x)	Octadecylamine/HCl	HCl	Oc(0.5)	1st method
Sap-3AM(0.5)–HCl(x)	3-Aminopropyltriethoxysilane/HCl	HCl	3AM(0.5)	1st method
Sap-Oc(0.5)–3AM(x)	Octadecylamine/3-aminopropyltriethoxysilane	3AM	Oc(0.5)	1st method
Sap-Oc(0.5)–3AM(0.5)–HCl(x)	Octadecylamine/3-aminopropyltriethoxysilane/HCl	HCl	Oc(0.5), 3AM(0.5)	1st method
Sap-Tr(x)	Trimethyloctadecylammonium bromide	Tr		1st method
Sap-Tr(0.5)–HCl(x)	Trimethyloctadecylammonium bromide/HCl	HCl	Tr(0.5)	1st method
Sap-TEOS(x)–3AM(3)	TEOS/3-aminopropyltriethoxysilane	TEOS	3AM(3)	2nd method
Sap-TEOS(5)–3AM(x)	TEOS/3-aminopropyltriethoxysilane	3AM	TEOS(5)	2nd method

The samples Sap-Aq(0) and Sap-Tr(0) are the starting materials.
[a] The samples were prepared by adding the necessary amount of surfactant to obtain 0, 0.5, 1, 2 and 5 times the CEC of the clay.

Table 2
Nomenclature and preparation conditions of the titanium modified saponites synthesized.

Sample[a]	Titanium source	Nomenclature[b]
Sap-TEOS(5)–3AM(3)-Ti6	Titanium (IV) bis(ammonium lactate) dihydroxide ($[CH_3CH(O-)CO_2NH_4]_2Ti(OH)_2$, $C_6H_{18}N_2O_8Ti$)	Sap-Ti6
Sap-TEOS(5)–3AM(3)-Ti8	Titanium (IV) ethoxide ($Ti(OC_2H_5)_4$, $C_8H_{20}O_4Ti$)	Sap-Ti8
Sap-TEOS(5)–3AM(3)-Ti12	Titanium (IV)-isopropoxide ($Ti[OCH(CH_3)_2]_4$, $C_{12}H_{28}O_4Ti$)	Sap-Ti12
Sap-TEOS(5)–3AM(3)-rutile	TiO_2, rutile	Sap-Ti

[a] The sample Sap-TEOS(5)–3AM(3) was prepared by adding tetraethoxysilane (TEOS) and 3-aminopropyltriethoxysilane (3AM) to obtain 5 and 3 times the cation exchange capacity (CEC) of the saponite.
[b] The number of the C atoms of the titanium source is included in the nomenclature.

25 kV over samples in which a thin gold layer was deposited by evaporation using a Bio-Rad ES100 SEN coating system.

3. Results and discussion

3.1. Effect of the organic surfactant

3.1.1. X-ray diffraction

The XRD patterns of the solids with the largest basal spacings obtained when treating Sap with each type of organo-modifier are presented in Fig. 1. In this figure, the amount of organo-modifier in each intercalated Sap is not the same. The d(001) reflection showed a basal spacing of 1.17 nm for the treated Sap (0.96 nm without intercalated water, for the TOT layer (Moore and Hower, 1986)), increasing this value until 3.60 nm in the case of the sample functionalized with Arquad 2HT-75 (S-Aq(5)). A basal spacing of 3.60 nm implied that the interlayer region had a height about 2.65 nm, which means that the surfactant molecules adopt a paraffin-type arrangement. In the cases of trimethyloctadecylammonium bromide (S-Tr(2)) and 3-aminopropyltriethoxysilane + tetraethoxysilane (S-TEOS(5)–3AM(3)), the OC had basal spacings of 1.92 and 1.90 nm, respectively, which reflected an arrangement of the surfactant molecules intermediate between lateral-bilayer and pseudotrimolecular layer structure. When octadecylamine and 3-aminopropyltriethoxysilane (S-Oc(0.5)–3AM(5)) were used together to functionalize the Sap, the basal spacing found is 1.75 nm, suggesting a lateral-bilayer arrangement. Samples S-3AM(0.5)–HCl(5) and S-Oc(0.5)–HCl(5) were synthesized in the presence of hydrochloric acid, and the basal spacings obtained were 1.47 and 1.42 nm, meaning a lateral monolayer arrangement.

The effect of the amount of surfactant added in the basal spacing of the Sap is presented in Fig. 2. All the samples considered were synthesized without the addition of HCl. For S-Aq(x) and S-Tr(x) the level of loading can increase beyond reaching the maximum basal spacing. After reaching the largest value of basal spacing for each sample, the amount of surfactant further fixed did not cause additional layer swelling. The fixation of further amounts of the surfactants after reaching the maximum basal spacing might be due to the fact that a small amount of surfactant occupied the external surface of the clay particles (He et al., 2006a,2006b; Hedley et al., 2007; Juang et al., 2002) or because some molecules of the surfactants can still package in the interlayer space, although without increasing the separation between the layers. The number of C atoms in the alkyl chain had a great effect on the basal spacing. Arquad 2HT-75 and trimethyloctadecylammonium have the same alkyl chain length (C_{18}), but the first one has two long chains while the second surfactant only one. The basal spacing of Sap modified with Arquad 2HT-75 was markedly higher, up to 3.60 nm, than those of organo-Sap modified with trimethyloctadecylammonium (1.90 nm), in accordance with previously reported results (He et al.,

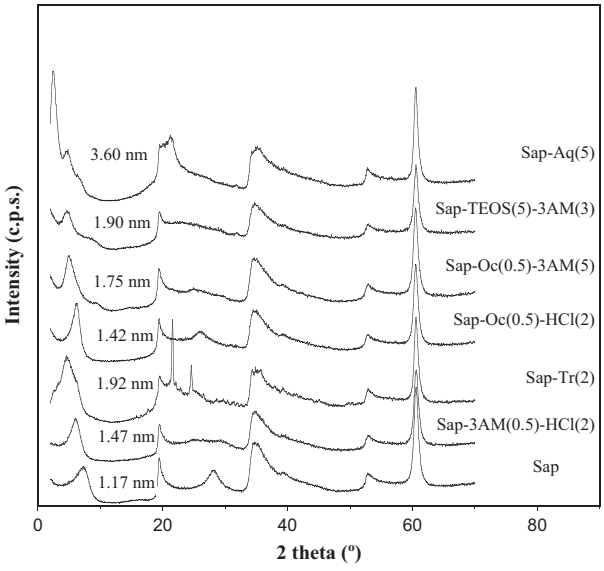

Fig. 1. XRD patterns of the saponite and selected surfactant–saponite solids. The basal spacings from the d(001) reflection are also included.

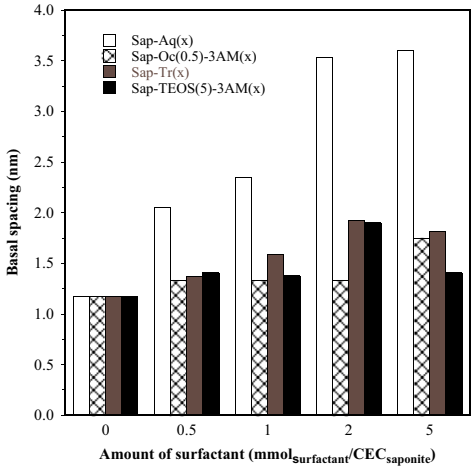

Fig. 2. Effect of the amount of surfactant added in the basal spacing of the surfactant–saponite solids.

2010). The two long chains are bonded to the N atom occupying two vertices of a tetrahedron, and although the free rotation of C – C single bonds may allow them to adopt different dispositions, the very large basal spacing of the intercalated solids made clear that these chains may remain almost in opposite directions. In the cases in which the intercalation was done using two surfactants, the relationship between the amount of surfactant and the d(001) value was not clear. However, the basal spacing of S-Oc(0.5)–3AM(x) and S-TEOS(5)–3AM(x), when the amount of 3-aminopropyltriethoxysilane is 5 CEC, was almost the same (1.7 nm) in both samples.

The last group of solids was composed of the samples synthesized by adding variable amounts of hydrochloric acid and with a fixed amount of surfactant (0.5 CEC). All of these samples presented basal spacings between 1.23 and 1.54 nm, which suggested a monolayer arrangement of surfactant in the interlayer space of Sap. It was observed that the addition of hydrochloric acid had no significant effect in the basal spacing.

3.1.2. Chemical analysis

The chemical composition of all the samples and the amount of organic matter incorporated to the solids are shown in Table 3. These compositions have been referred to water-free solids, that is, the content of metallic oxides and carbon was normalized to 100%.

Table 3
Water-free chemical composition (mass%) of natural and intercalated samples.[a,b]

Sample	SiO_2	Al_2O_3	CaO	MgO	Na_2O	C
Sap	58.72	5.30	0.389	31.72	3.83	–
Sap-Aq(0.5)	44.10	3.68	0.404	23.91	0.70	27.18
Sap-Aq(1)	41.02	3.36	0.383	22.13	0.42	32.66
Sap-Aq(5)	32.78	2.44	0.314	17.61	0.43	46.40
Sap-Aq(0.5)–HCl(0.5)	49.20	4.18	0.351	26.45	0.35	19.44
Sap-Aq(0.5)–HCl(5)	53.88	3.34	0.332	20.85	0.23	21.35
Sap-Oc(0.5)–HCl(5)	64.58	4.36	0.352	25.82	0.17	4.69
Sap-3AM(0.5)	59.45	4.92	0.503	31.31	2.35	1.45
Sap-3AM(0.5)–HCl(5)	66.90	4.47	0.387	26.70	0.40	1.12
Sap-Oc(0.5)–3AM(0.5)	56.46	4.52	0.430	29.83	1.99	6.74
Sap-Oc(0.5)–3AM(5)	58.92	4.05	0.410	25.57	0.18	10.83
Sap-Oc(0.5)–3AM(0.5)–HCl(5)	65.15	4.30	0.324	25.63	0.25	4.30
Sap-Tr(0.5)	52.60	4.27	0.419	28.68	1.05	12.94
Sap-Tr(2)	38.62	3.00	0.340	20.88	0.63	36.50
Sap-TEOS(5)	65.07	3.82	0.402	26.26	3.51	0.91
Sap-TEOS(5)–3AM(3)	64.20	3.03	0.363	19.04	2.37	10.97

[a] Water-free composition was calculated by normalizing the content of metallic oxides and carbon to 100%. Thus, water content, and also the amount of N and H in the organic surfactants were ignored.

[b] Fe_2O_3, K_2O and TiO_2 contents were always <0.15%, and they were also omitted in the normalized composition.

The amount of organic matter present in the samples varied a lot, reaching values near 50% in some cases. In this term, for the same type of surfactant, if the amount of organic molecule added in the synthesis increased, also the amount of organic matter fixed by the sample grew. Moreover, in accordance with the effect shown by XRD, the increase of the amount of surfactant led to an increasing basal spacing. Most of the samples lost almost all of the initial Na_2O, Na^+ being the main exchangeable cation in natural clay mineral, suggesting that the incorporation of surfactants mainly happened by a cation exchange process. It is remarkable that the amount of CaO remained practically constant, indicating that Ca^{2+} was not an exchangeable cation, and suggesting that it was in the clay mineral in the form of an insoluble impurity, probably feldspar, not detected by XRD.

Samples that had been synthesized with a HCl/clay mineral ratio of 5 meq/g exhibited a decrease on Mg^{2+} content of about 5% (see Table 3). This fact may be due to the capacity of the acid to easily dissolve part of the clay structural magnesium (Vicente Rodríguez et al., 1996). Increased SiO_2 percentage did not directly mean an increase of the amount of this element in the clay mineral; it was a consequence of magnesium decrease (Pérez-Santano et al., 2005). Only in the samples treated with 3-aminopropyltriethoxysilane and/or TEOS part of this increase was due to the surfactants fixed by the clay mineral. For S-TEOS(5), the contribution of the incorporation of TEOS to the increase in SiO_2 content was clearly shown.

The strong variation of metallic oxides from one sample to others was mainly due, as indicated, to the organic matter fixed by the solids and thus, the effects caused by the treatments in the chemical composition of the clay mineral were masked. This can be solved referring the chemical composition to an "internal patron" in the clay mineral, and SiO_2 is usually employed, as the amount of this element remains constant during several treatments. In the present case, SiO_2 content cannot be used as reference for the solids obtained by treatment with 3-aminopropyltriethoxysilane or TEOS, as they incorporated SiO_2 to the solids, the normalization of the other solids to the SiO_2 content in the parent Sap is given in Table 4. Thus, when maintaining the amount of the clay mineral treated, the amount of carbon fixed increased up to 83.12 mass% in sample S-Aq(5). The octahedral layer of the clay mineral was relatively affected when the treatments were carried out under acid conditions and remained practically unaltered when HCl was not used, as can be seen from the evolution of Al_2O_3 and MgO contents. Thus, up to 31.3% of the initial Al^{3+} and up to 28.4% of initial Mg were dissolved, both in S-Aq(0.5)–HCl(5), one of the samples prepared with higher HCl amount.

As indicated, the composition of the solids obtained by treatment with 3-aminopropyltriethoxysilane and TEOS cannot be normalized to SiO_2 content. Unfortunately, it was not possible to find an internal reference in these solids, as both Mg^{2+} and Al^{3+} were dissolved in important amounts, mainly in the synthesis using HCl. In any case, the increases of

Table 4
Chemical composition of the samples, normalized to the SiO_2 content in the parent saponite.[a]

Sample	SiO_2	Al_2O_3	CaO	MgO	Na_2O	C
Sap	58.72	5.30	0.389	31.72	3.83	–
Sap-Aq(0.5)	58.72	4.90	0.538	31.84	0.93	36.19
Sap-Aq(1)	58.72	4.81	0.548	31.68	0.60	46.75
Sap-Aq(5)	58.72	4.37	0.562	31.54	0.77	83.12
Sap-Aq(0.5)–HCl(0.5)	58.72	4.99	0.400	31.57	0.42	23.20
Sap-Aq(0.5)–HCl(5)	58.72	3.64	0.362	22.72	0.25	23.27
Sap-Oc(0.5)–HCl(5)	58.72	3.96	0.320	23.45	0.15	4.26
Sap-3AM(0.5)	58.72	4.86	0.497	30.92	2.32	1.43
Sap-3AM(0.5)–HCl(5)	58.72	3.92	0.340	23.43	0.35	0.98
Sap-Tr(0.5)	58.72	4.77	0.468	32.02	1.17	14.45
Sap-Tr(2)	58.72	4.56	0.517	31.75	0.96	55.50

[a] The composition of the samples obtained by treatment with 3-aminopropyltriethoxysilane and tetraethoxysilane is not included, as the treatment incorporated SiO_2 to the solids.

Table 5
Thermal analyses of saponite and organoclays.

Sample	Dehydration	Surfactant elimination			Dehydroxylation	
	Water content (%)	Onset temperature of decomposition (°C)	Organic content (%)	DTG peaks (°C)	Onset temperature (°C)	Mass loss (%)
Sap	11.3				694	3.0
Organoclay						
Sap-Aq(0.5)	3.30	229	27.4	327/418	513	2.33
Sap-Aq(1)	2.55	193	32.55	320/415	509	2.80
Sap-Aq(5)	2.39	163	46.06	294/401	445	3.94
Sap-Aq(0.5)–HCl(0.5)	4.48	192	20.25	328/414	502	3.42
Sap-Aq(0.5)–HCl(5)	4.12	210	21.89	335/422	530	2.54
Sap-Oc(0.5)	4.34	139	21.79	238/414	498	3.59
Sap-Oc(0.5)–HCl(5)	11.64	200	6.35	258/382	421	3.54
Sap-3AM(0.5)	13.32	387	0.54	412	436	2.92
Sap-3AM(0.5)–HCl(5)	15.03	367	1.42	413	463	3.37
Sap-Oc(0.5)–3AM(0.5)	8.33	327	6.36	411	485	2.36
Sap-Oc(0.5)–3AM(5)	5.43	260	11.8	375/426	530	3.69
Sap-Oc(0.5)–3AM(0.5)–HCl(5)	11.91	270	4.77	367	476	2.97
Sap-Tr(0.5)	3.91	279	14.04	394	520	2.85
Sap-Tr(2)	2.59	167	38.94	238/404	217	2.41
Sap-Tr(0.5)–HCl(5)	6.79	241	11.15	416/512	538	3.06
Sap-TEOS(5)	13.39	200	8.02		459	3.86
Sap-TEOS(5)–3AM(3)	9.22	297	11.67	442	662	2.36
Titanium organoclay						
Sap-Ti6	8.13	266	28.63	277	615	3.00
Sap-Ti8	7.82	228	11.37	230	638	2.32
Sap-Ti12	14.81	103	15.76	–	539	3.05
Sap-Ti	4.57	214	12.06	359/777	612	0.34

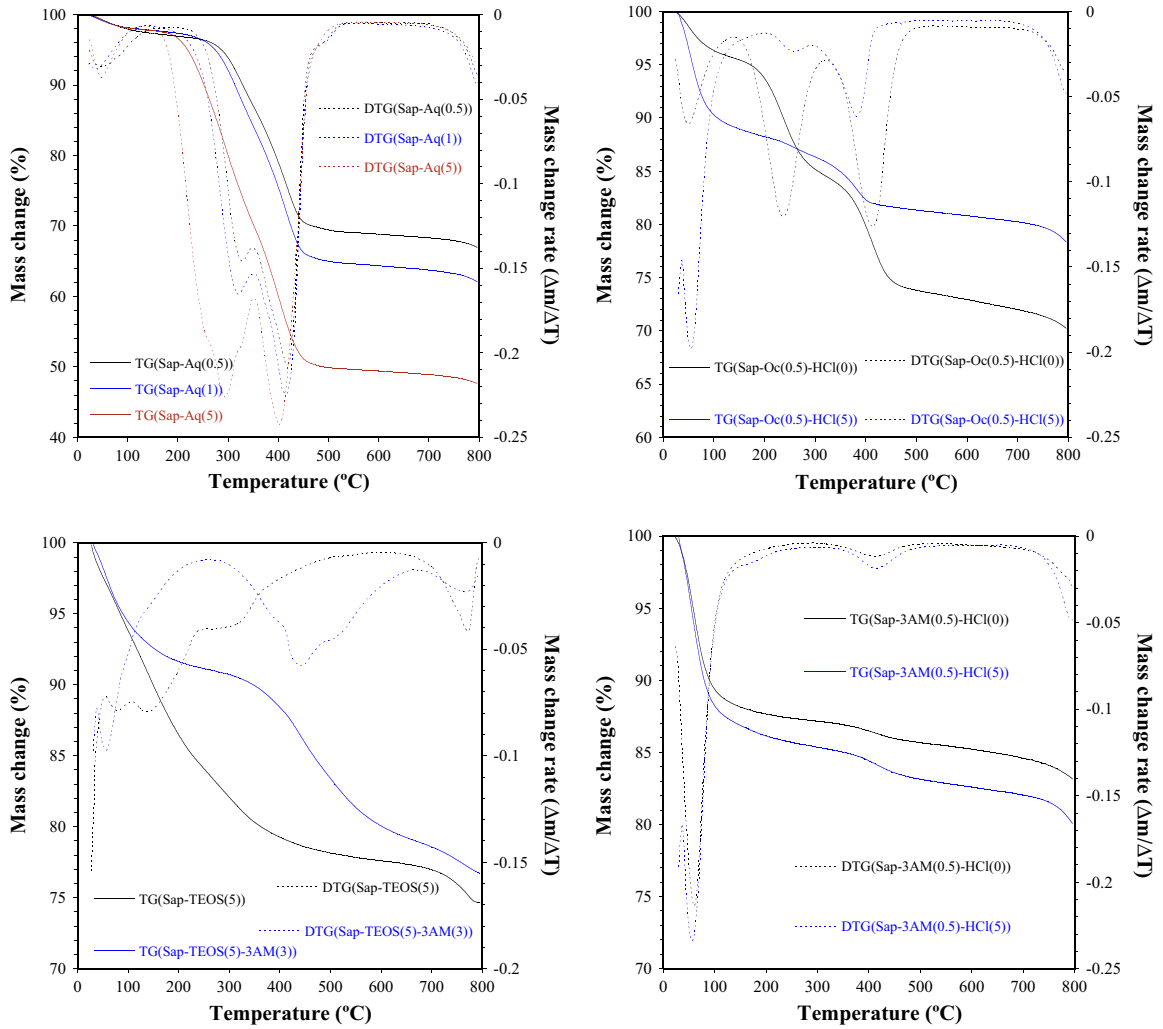

Fig. 3. Thermogravimetric curves of selected samples.

Table 6
Assignment of the IR absorption bands (cm^{-1}) of saponite and organoclays.

Assignment	Sap	Aq	Oc	3AM	Oc + 3AM	Tr	TEOS + 3AM
ν O–H (MgOH)	3676	3676	3676	3676	3676	3676	3676
ν O–H (H_2O)	3464	3464	3464	3464	3464	3464	3464
ν C–H	2962–2864	2962–2864	2962–2864	2962–2864	2962–2864	2962–2864	2962–2864
δ H_2O	1636	1636	1636	1636	1636	1636	1636
N–H		1490	1468	1664–1460	1464	1472	1600–1300
Si–O–Si	1004	1004	1004	1004	1004	1004	1004
Si–O–Si			478				
Si–O–Mg	446	446	446	446	446	446	446

SiO_2 content were clearly observed from the water-free compositions given in Table 3, and these increases would be even higher considering the dissolution of the rest of the cations of the clay mineral.

3.1.3. Thermal analysis

Results of the thermogravimetric analyses are summarized in Table 5, while the curves of some selected samples are given in Fig. 3. Several mass loss steps were found in each sample. A mass-loss step was observed from room temperature to near 200 °C due to dehydration of adsorbed water and was also attributed to dehydration of water coordinated to metal cations. A second mass-loss step was observed in the temperature range 200 to 600 °C and was due to the evolution of the organic substances. Finally, above 600 °C, the third mass-loss step was ascribed to the dehydroxylation of the structural OH units of the clay mineral (Xi et al., 2004). In the case of the synthetic Sap, a strong mass loss is observed from 20 to 170 °C of about 8.64%, due to the loss of adsorbed water, a second step of mass loss but with a gentle slope from 170 to 695 °C (2.68%), and above 695 °C the loss of structural hydroxyl groups (3.0%) followed by the transformation of the clay mineral to enstatite (Avila et al., 2010).

Compared to the Sap, OC had lower decreases in water content in the first step. This observation can be explained in terms of the hydrophobic nature of the surfactants. The residual water molecules in the OC were located in the interlayer region, between the surfactant ions. The substitution of the original inorganic compensating cations by organic cations made that the water initially bonded to the inorganic cations did not remain in the treated solids. Moreover, the samples that had been synthesized with the addition of HCl had more water content than those prepared using only the surfactants. This fact may be due to the capacity of HCl to modify the clay mineral surface making it more able to adsorb water molecules. In the second mass loss step, corresponding to the decomposition of the organic matter contained in the Sap, the onset temperature depended on the kind of surfactant. The lowest onset was 139 °C and corresponded to octadecylamine, while Arquad 2HT-75 had its onset at about 229 °C and trimethyloctadecylamine began to decompose at 279 °C. Finally, samples which had been synthesized using 3-aminopropyltriethoxysilane had their onset temperatures near 300 °C. These samples had the highest onset temperatures, confirming that the alkylsilane chains, which formed stable siloxane bridges with the Sap surface, provided additional thermal stability (Ruiz-Hitzky and Van Meerbeek, 2006). The thermal stability of organic matter decreased as the amount of intercalated surfactant increased (Hedley et al., 2007). For example, in the case of Arquad 2HT-75, for the partially exchanged Arquad-Sap (S-Aq(0.5)) the onset temperature was 229 °C, the sample S-Aq(1) began to decompose at 193 °C and for S-Aq(5) this temperature decreased until 163 °C.

With respect to the mass loss in the temperature range 200–600 °C, it increased with the size of the organic cation from 0.54% (S-3AM(0.5)) to 46.06% (S-Aq(5)). DTG curves established how many steps, between one and three, composed the second mass-loss process. In samples S-Aq, S-Oc and S-Oc–3AM, two peaks appeared in their DTG curves, suggesting that the molecules were successively broken in different fragments or that the molecules were located in environments with different accessibility, as in the pores between clay particles in the interlayer space.

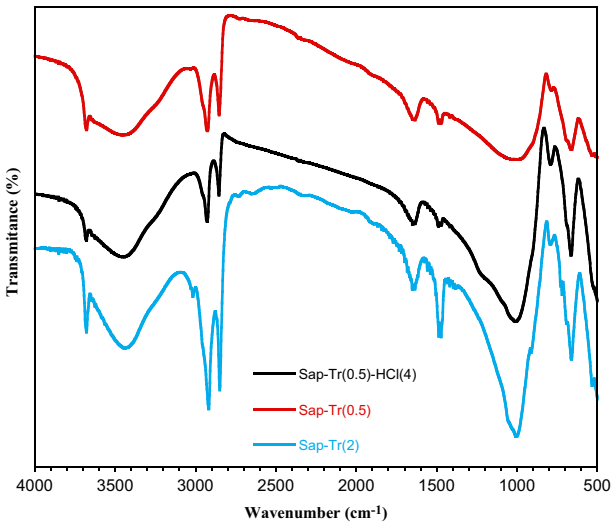

Fig. 4. FTIR spectra of the saponite modified with trimethyloctadecylammonium bromide.

3.1.4. Fourier transform infrared spectroscopy

The IR spectra of the OC consisted of the absorption bands related to the vibrations of the characteristic groups of Sap and the corresponding organic species. A summary of the assignment of the different bands is presented in Table 6. The spectrum of synthetic Sap exhibited two peaks at high wavenumbers: the O–H stretching vibration mode of MgO–H appeared at 3676 cm^{-1} and the stretching of water O–H groups was observed at 3464 cm^{-1}. In the middle region, the bending band of water appeared near 1636 cm^{-1} and the Si–O–Si vibration mode was observed at 1004 cm^{-1}. The bands situated at lower wavenumbers, due to the vibrations of Si–O–Al and Si–O–Mg, were located at 600 and 446 cm^{-1} (Vicente Rodríguez et al., 1996). The infrared spectra of the OC were very similar to the Sap but included some differences. As example, the spectra for the samples S-Tr are shown in Fig. 4. The O–H stretching vibration mode was much more intense in functionalized samples. The increase in intensity of this mode may be due to the exclusion or water molecules from the clay mineral, suggesting an interaction of the amines with OH groups of the clay mineral (this interaction was similar with siloxane groups in samples treated with the alkoxides). A new peak appeared in the middle region near 1470 cm^{-1} due to the vibrations of N–H bonds of the organic molecules. In the case of the surfactants which contained Si–O bonds, their vibration modes were masked by those of Sap (Avila et al., 2010; Jankovic et al., 2011; Ruiz-Hitzky and Van Meerbeek, 2006; Xi et al., 2004).

3.1.5. Scanning electron microscopy

The textural changes induced by the functionalization are shown in Fig. 5, in which SEM micrographs and EDX analysis of two OC are compared to the Sap. The pristine clay had curved plates with size between 5

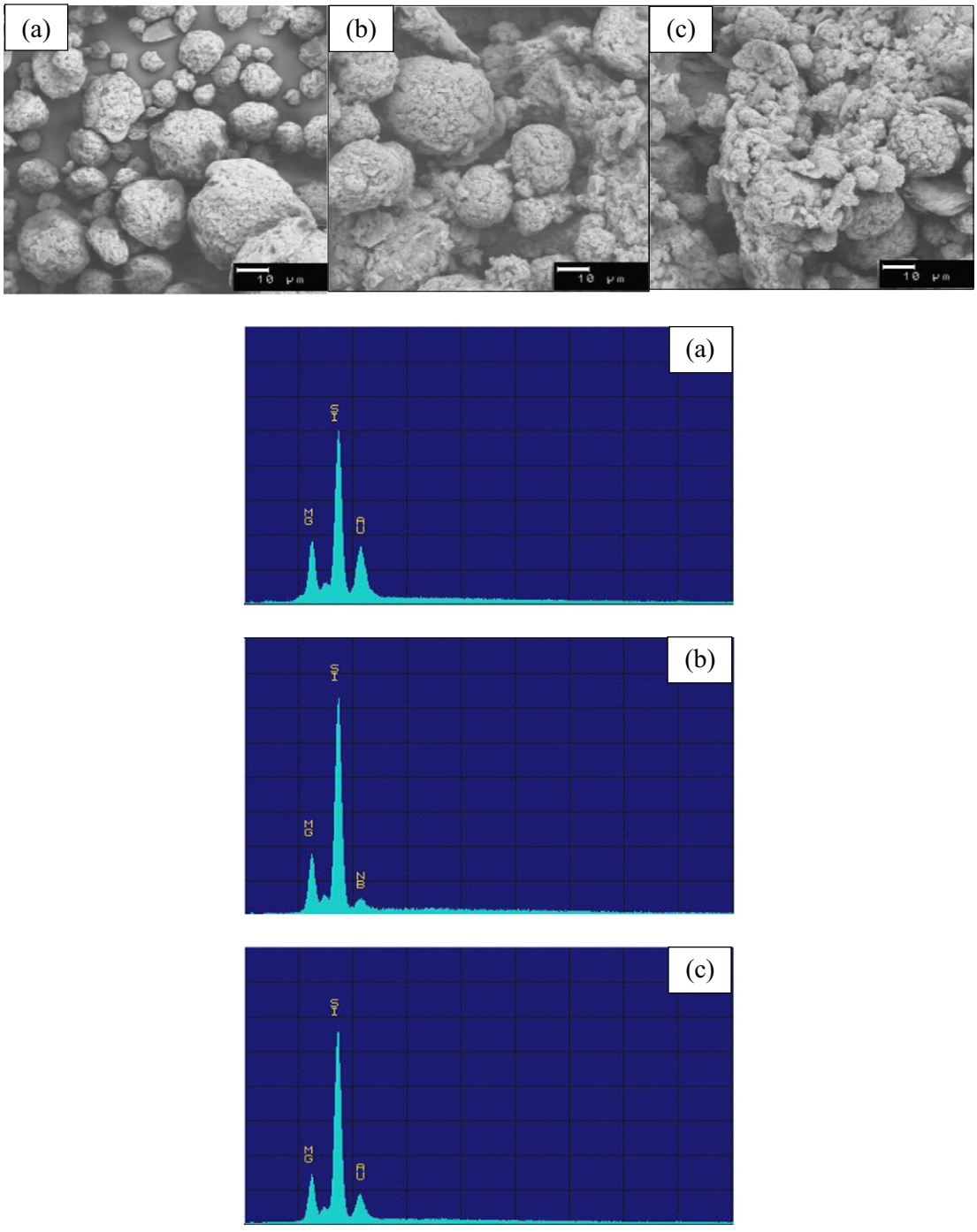

Fig. 5. SEM micrographs and EDX analysis of the synthetic saponite (a) and the samples Sap-Oc(0.5)–3AM(5) (b) and Sap-3AM(0.5)–HCl(5) (c).

and 20 µm. However, the functionalized solids showed significant changes in the morphology. Compared to the morphology of Sap, the particles grew and became relatively flat. Besides, the particles became clearly spongier (see micrographs related to samples S-Oc(0.5)–3AM(5) and S-3AM(0.5)–HCl(5)). Moreover, the increase of the amount of surfactant fixed by the clay mineral caused the increment of the particle size, reaching 200 µm (He et al., 2006a). The characteristic of the samples that had been synthesized with the addition of hydrochloric acid was that their particles were very small and tended to form aggregates. As discussed in the previous sections, the effect of acid is twofold; firstly, it modifies the surface allowing that the clay mineral is able to absorb more water and it is capable of partially dissolving the octahedral clay layer. In this case, it affects the size of the observed particles. From the EDX analysis carried out in these samples, and also included in Fig. 5, no phase segregation or particles with high concentration of SiO_2 were found.

3.2. Effect of the titanium surfactant

3.2.1. X-ray diffraction

The XRD patterns of the titanium OC are presented in Fig. 6. In this figure, the diffractograms of the titanium OC non-calcined were very similar to that obtained for the reference samples, Sap and S-TEOS(5)–3AM(3). The diffraction peaks at 25.3, 37.8, 48.1, 53.8 and 55.1° observed for the calcined samples corresponded to TiO_2 under anatase form (see for example the pattern of S-Ti8 calcined sample included in

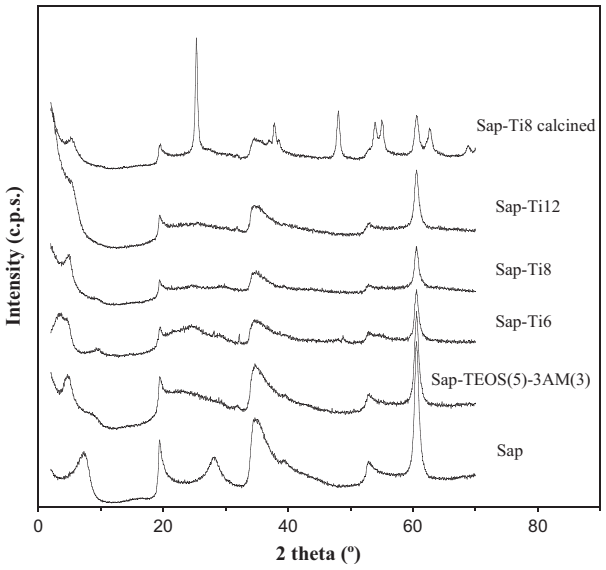

Fig. 6. XRD patterns of the synthetic saponite and titanium surfactant–saponite solids.

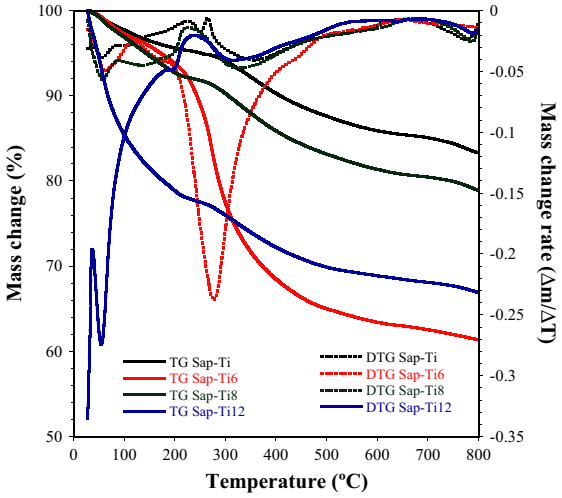

Fig. 7. Thermogravimetric curves of the modified titanium saponites.

the figure). No peaks from other titanium species were detected for any of the calcined samples.

3.2.2. Chemical analysis

The chemical compositions of titanium OC are shown in Table 7. The amount of organic matter present in the samples varied between 8.90 and 20.30%, related to the amount of titanium precursor added in the modification of Sap. The TiO_2 content in the samples ran parallel, being between 14.25 and 26.84%.

3.2.3. Thermal analysis

The results of the thermogravimetric analyses of the non-calcined samples are summarized in Table 4, while the curves are given in Fig. 7. Compared to the Sap and the reference sample S-TEOS(5)–3AM(3), titanium OC did not have the same behavior in water content in the first step, from room temperature to near 200 °C. S-Ti, S-Ti6 and S-Ti8 had lower mass losses than S-Ti12. For these samples, the major difference appeared in the temperature range 200–600 °C where the sample S-Ti6 presented a significant mass loss associated to the decomposition of ammonium lactate. In the case of the calcined samples (not included), no significant mass losses were observed throughout the whole range of temperatures.

3.2.4. Fourier transform infrared spectroscopy

The IR spectra of the non-calcined samples are presented in Fig. 8-a. The spectra of these samples were similar. In the region of high wavenumbers, a peak appeared at 3676 cm^{-1} corresponding to the stretching vibration mode of the SiO – H bonds. Near to this peak, a shoulder appeared at 3460 cm^{-1}, attributed to the absorbed water. Also in this region, two peaks located at 2854 and 2926 cm^{-1} due to the symmetric and antisymmetric vibrations of the CH bonds were shown. Major differences arose in the intermediate region. First, a peak appeared in all the samples at 1636 cm^{-1}, which was attributed to the water molecules located in the interlayer space. The intensity of this peak greatly varied from one sample to another. It may be

Table 7
Chemical composition (mass%) of titanium samples.[a]

Sample	SiO_2	Al_2O_3	TiO_2	MgO	Na_2O	C	N
Sap-Ti	47.20	2.70	14.25	15.32	1.02	8.90	–
Sap-Ti6	29.68	1.61	21.34	9.04	0.74	18.51	18.67
Sap-Ti8	49.43	2.88	17.48	15.83	1.79	11.96	0.16
Sap-Ti12	36.81	2.02	26.84	11.34	2.04	20.30	0.17

[a] Fe_2O_3, CaO, MnO and K_2O contents were always <0.15%, and they are omitted in the composition.

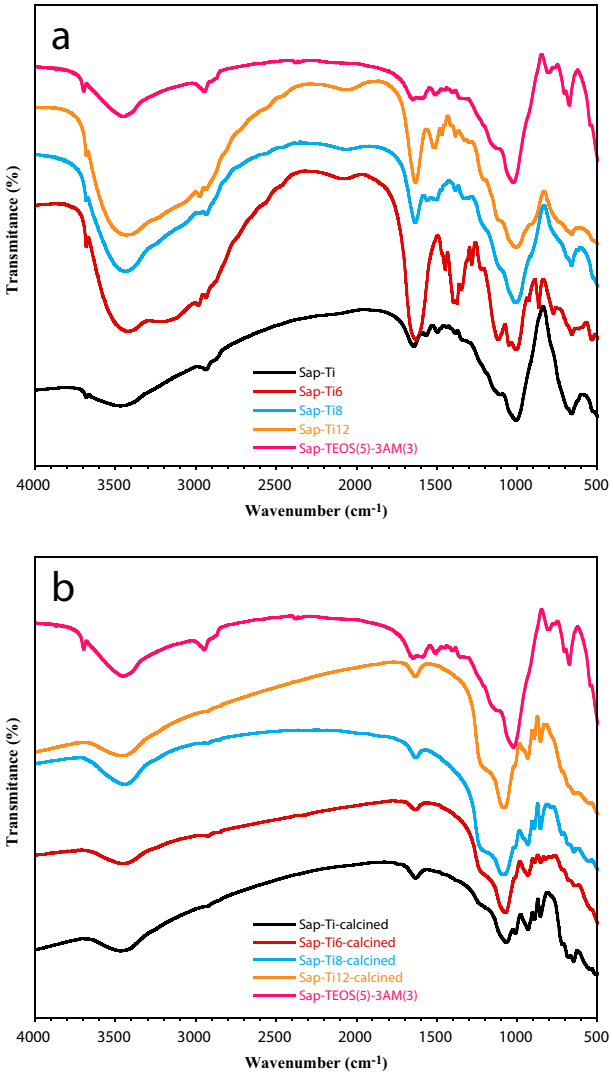

Fig. 8. FTIR spectra of the modified titanium saponites.

considered that at a very close wavenumber, 1640 cm^{-1}, is found in the vibration modes corresponding to NH bond. This result was consistent since S-Ti6 sample, which showed the most intense peak, contained NH bonds. Another characteristic peak of this bond appeared at 1460 cm^{-1}, being also visible in the latter sample. Finally, in the low region of the spectrum, a peak at a wavenumber of 1004 cm^{-1} highlighted, corresponding to the antisymmetric stretching vibration mode of Si – O – Si. A peak common to all samples appeared at 650 cm^{-1}, being attributed to vibrations of the Ti – O – Ti structures.

The IR spectra of the calcined samples are presented in Fig. 8-b. In these spectra, the peaks corresponding to the C – H bonds, located in the spectra at 2854 and 2926 cm^{-1}, disappeared. In addition, the region of low wavenumbers was modified, compared to the same region in the non-calcined samples, which may be due to a change in the structure of the clay produced by the calcination process.

3.2.5. Scanning electron microscopy

The textural changes induced by the treatments with the titanium precursors are shown in Fig. 9, in which SEM micrographs of the calcined samples S-Ti, S-Ti6, S-Ti8 and S-Ti12 are compared. The presence of the surfactants caused significant changes in the Sap morphology (see also Fig. 5), but there were no significant differences among the various samples treated with titanium. These samples formed particles clearly spongier.

3.3. Effect on the thermal stability of the saponite PVC nanocomposites

The evaluation of the thermal stability of synthesized nanocomposites was conducted as specified in the ISO 305:1990 standard. The studied samples included both non-calcined and calcined titanium OC. This standard specifies two methods to determine the thermal stability of PVC, and chlorinated polymers in general, by the color change that occurs when the samples are exposed, in sheet form, at elevated temperatures. The first method evaluates the color development at several intervals of time, for a given temperature. In this work, the experimental temperature was 180 °C and sampling in the time interval between 0 and 60 min. The results are shown in Fig. 10. The samples were not colored initially and all them had the same whitish color as the PVC. Taking into account the behavior of the PVC reference, the sample more resistant to color change was PVC/S-Ti6. The samples synthesized using calcined titanium OC showed some thermal resistance, with respect to the PVC reference. In the second method studied the temperature was reduced to 70 °C and the time was increased up to 7 days. The results are presented in Fig. 11, showing that with the exception of the sample PVC/S-Ti12, the synthesized samples have high resistance to the thermal aging. These results could be used as the starting point to continue developing the related resistance to UV radiation in our laboratories.

4. Summary and conclusions

In this work, a combination of techniques was used to characterize organo-Sap with several surfactants. XRD patterns indicated that all the solids had higher basal spacings than the natural clay mineral. The efficiency of the intercalation depended on the type of surfactant, i.e., the basal spacing increased with the alkyl chain length and for a given chain length, this space increased more if surfactant had two long chains instead of one. Moreover, it also depended on the surfactant/clay mineral ratio, the basal spacing increased with surfactant loading, good results being obtained in the range 2–5 meq/g of clay mineral. Otherwise, the HCl/clay mineral ratio did not influence the process. The intercalation efficiency of the surfactants used decreased in the order: Arquad 2HT-75 > trimethyloctadecylammonium bromide > TEOS + 3-aminopropyltriethoxysilane > octadecylamine +3-aminopropyltriethoxysilane > 3-aminopropyltriethoxysilane > octadecylamine.

Thermal analysis demonstrated that the onset temperature depended on the type of surfactant and, for a given surfactant, this stability decreased when increasing the surfactant loading. Samples which had been synthesized using 3-aminopropyltriethoxysilane had the highest onset temperature, confirming that the alkylsilane chain, which formed stable siloxane bridges with Sap surface, provided added thermal stability.

FT-IR analysis showed evidence of organophilization of all samples through the absorption bands due to the vibration of the C – H and N – H bonds corresponding to the organic modifiers. Other confirmation of functionalization was the presence of carbon in chemical analysis, the amount of organic material reaching values up to 45%. Moreover, this

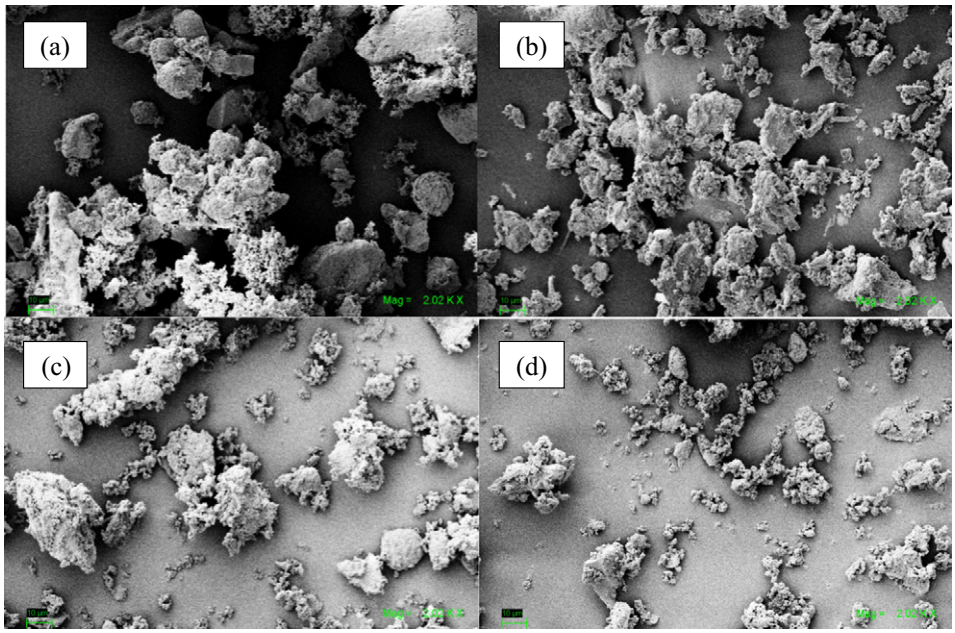

Fig. 9. SEM micrographs of the modified titanium saponites calcined. (a) Sap-Ti, (b) Sap-Ti6, (c) Sap-Ti8, (d) Sap-Ti12.

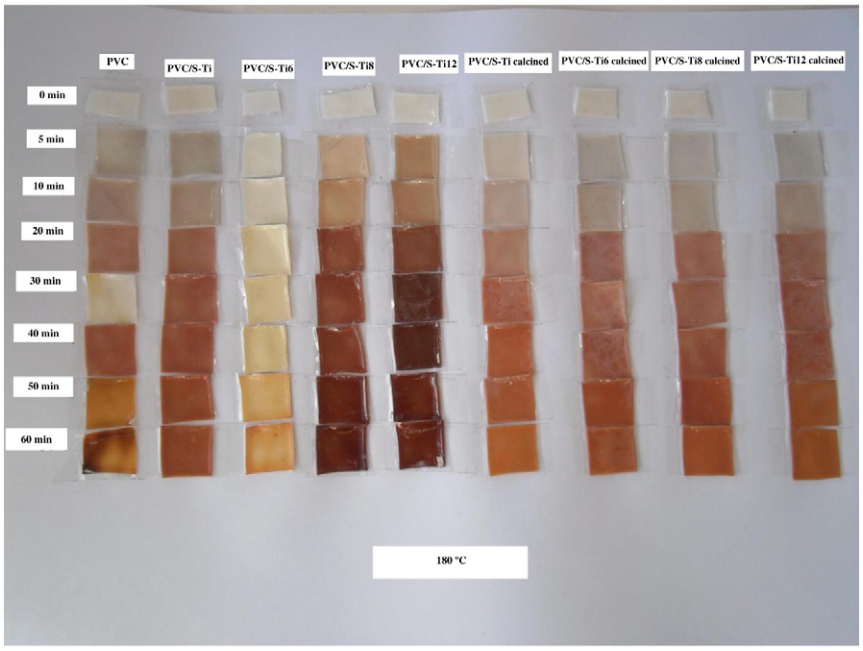

Fig. 10. Evolution with time, at 180 °C, of the color of titanium organoclay PVC nanocomposites.

analysis confirmed that when hydrochloric acid was added during the organophilization process, it removed part of the clay structural magnesium and aluminum. SEM micrographs demonstrated that the morphology of the OC depended on HCl addition. Samples synthesized without adding acid had their particles more angular and bigger than those from samples prepared with HCl which were smaller, rounded and tended to form aggregates.

In order to synthesize Sap-PVC nanocomposites with improved properties with respect to the initial PVC, the sample S-TEOS(5)–3AM(3) was used as reference to incorporate various titanium organic precursors to the polymer. The effect of temperature on the initial properties of the titanium modified Sap was studied at 60 and 850 °C. Only in the samples treated at 850 °C, the presence of TiO_2 was detected under anatase form by XRD. PVC/S-Ti6 sample, synthesized using titanium (IV) bis(ammonium lactate) dihydroxide as titanium source, showed more resistance to color change, considering the thermal stability at 180 °C for several times. When the temperature was 70 °C, all the samples were stable.

Acknowledgments

This work was funded by the Spanish Ministry of Science and Innovation (MICINN) and the European Regional Development Fund (FEDER) (project IPT-420000-2010-015).

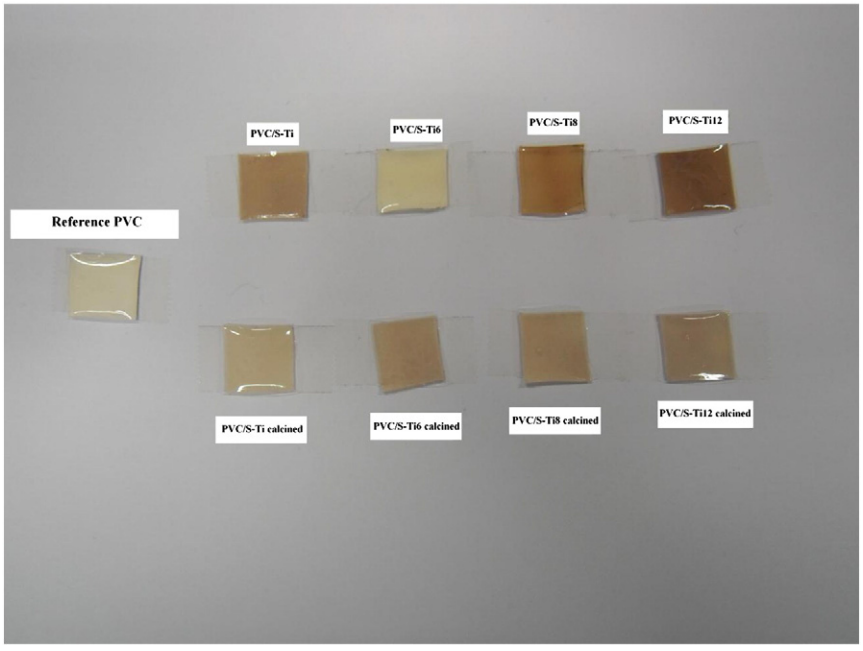

Fig. 11. Thermal resistance of the titanium organoclay PVC nanocomposites at 70 °C for 7 days.

References

Avila, L.R., de Faria, E.H., Ciuffi, K.J., Nassar, E.J., Calefi, P.S., Vicente, M.A., Trujillano, R., 2010. New synthesis strategies for effective functionalization of kaolinite and saponite with silylating agents. J. Colloid Interface Sci. 341, 186–196.

Awad, W.H., Beyer, G., Benderly, D., Ijdo, W.L., Songtipya, P., Jimenez-Gasco, M.M., Manias, E., Wilkie, Ch.A., 2009. Material properties of nanoclay PVC composites. Polymer 50, 1857–1867.

Bergaya, F., Detellier, C., Lambert, J.F., Lagaly, G., 2013. Introduction to Clay–Polymer Nanocomposites (CPN), chapter 13, handbook of clay science, In: Bergaya, F., Lagaly, G. (Eds.), Developments in Clay Science, 2nd edition, vol. 5A. Elsevier, Amsterdam, pp. 655–677.

Betega de Paiva, L., Morales, A.R., Díaz, F.R.V., 2008. Organoclays: properties, preparation and application. Appl. Clay Sci. 42, 8–24.

Chen, B., Evans, J.R.G., Greenwell, H.C., Boulet, P., Coveney, P.V., Bowden, A.A., Whiting, A., 2008. A critical appraisal of polymer–clay nanocomposites. Chem. Soc. Rev. 37, 568–594.

Dunlap, L.H., Desch, R., 1982. Plastic building products. In: Mark, H.F., Othmer, D.F., Overberger, Ch.G., Seaborg, G.T. (Eds.), Kirk–Othmer Encyclopedia of Chemical Technology, vol. 18. John Wiley & Sons, New York, pp. 87–110.

Galimberti, M., Cipolletti, V.R., Coombs, M., 2013. Applications of clay–polymer nanocomposites, chapter 4.4, handbook of clay science, In: Bergaya, F., Lagaly, G. (Eds.), Techniques and Applications, 2nd edition, vol. 5B. Elsevier, Amsterdam, pp. 539–586.

Gesenhues, U., 2000. Influence of titanium dioxide pigments on the photodegradation of poly(vinyl chloride). Polym. Degrad. Stab. 68, 185–196.

Giannelis, E.P., 1996. Polymer layered silicate nanocomposites. Adv. Mater. 8, 29–35.

Gong, F., Feng, M., Zhao, Ch., Zhang, Sh., Yang, M., 2004. Thermal properties of poly(vinyl chloride)/montmorillonite nanocomposites. Polym. Degrad. Stab. 84, 289–294.

He, H.P., Frost, R.L., Bostrom, T., Yuan., P., Doung, L., Yang, D., Xi, Y.F., Kloprogge, T.J., 2006a. Changes in the morphology with HDTMA$^+$ surfactant loading. Appl. Clay Sci. 31, 262–271.

He, H.P., Zhou, Q., Martens, W.N., Kloprogge, T.J., Yuan, O., Xi, Y.F., Zhu, J.X., Frost, R.L., 2006b. Microstructure of HDTMA$^+$-modified montmorillonite and its influence on sorption characteristics. Clays Clay Minerals 54, 689–696.

He, H., Ma, Y., Zhu, J., Yuan, P., Qing, Y., 2010. Organoclays prepared from montmorillonites with different cation exchange capacity and surfactant configuration. Appl. Clay Sci. 48, 67–72.

Hedley, C.B., Yuang, G., Theng, B.K.G., 2007. Thermal analysis of montmorillonites modified with quaternary phosphonium and ammonium surfactant. Appl. Clay Sci. 35, 180–188.

Jankovic, L., Madejova, J., Komadel, P., Jochec-Moscobá, D., Chodák, I., 2011. Characterization of systematically selected organo-montmorillonites for polymer nanocomposites. Appl. Clay Sci. 51, 438–444.

Juang, R.S., Lin, S.H., Tsao, K.H., 2002. Mechanism of sorption of phenols from aqueous solution onto surfactant-modified montmorillonite. J. Colloid Interface Sci. 254, 234–241.

Kemp, T.J., McIntyre, R.A., 2006. Transition metal-doped titanium(IV) dioxide: characterisation and influence on photodegradation of poly(vinyl chloride). Polym. Degrad. Stab. 91, 165–194.

Lagaly, G., 1999. Introduction: from clay mineral–polymer interactions to clay mineral–polymer nanocomposites. Appl. Clay Sci. 15, 1–9.

Lambert, J.F., Bergaya, F., 2013. Smectites–polymer nanocomposites, chapter 13.1, handbook of clay science, In: Bergaya, F., Lagaly, G. (Eds.), Developments in Clay Science, 2nd edition, vol. 5A. Elsevier, Amsterdam, pp. 699–706.

LeBaron, P.C., Wang, Z., Pinnavaia, T.J., 1999. Polymer-layered silicate nanocomposites: an overview. Appl. Clay Sci. 15, 11–29.

Liu, J., Chen, G.M., Yang, J.P., 2008. Preparation and characterization of poly(vinyl chloride)/layered double hydroxide nanocomposites with enhanced thermal stability. Polymer 49, 3923–3927.

Moghri, M., Akbarian, M., 2009. Effects of nanoclay and additives on the fusion characteristics and thermal stability of poly(vinyl chloride) nanocomposites. J. Vinyl Additive Tech. 15, 92–98.

Moore, D.M., Hower, J., 1986. Ordered interstratification of dehydrated and hydrated Na–smectite. Clays Clay Minerals 34, 379–384.

Pavlidou, S., Papaspyrides, C.D., 2008. A review on polymer-layered silicate nanocomposites. Prog. Polym. Sci. 32, 1119–1198.

Peprnicek, T., Duchet, J., Kovarova, L., Malac, J., Gerard, J.F., Simonik, J., 2006. Poly(vinyl chloride)/clay nanocomposites: X-ray diffraction, thermal and rheological behaviour. Polym. Degrad. Stab. 91, 1855–1860.

Pérez-Santano, A., Trujillano, R., Belver, C., Gil, A., Vicente, M.A., 2005. Effect of the intercalation of a montmorillonite with octadecylamine. J. Colloid Interface Sci. 284, 239–244.

Pinnavaia, T.J., Beall, G.W., 2000. Polymer–Clay Nanocomposites. J. Wiley & Sons, Chichester.

Plastics—determination of thermal stability of poly(vinyl chloride), 2001. Plastics — determination of thermal stability of poly(vinyl chloride), related chlorine-containing homopolymers and copolymers and their compounds — discoloration method. European Committee for Standardization, Bruxelles.

Ruiz-Hitzky, E., Van Meerbeek, A., 2006. Clay mineral- and organo-clay–polymer nanocomposites, chapter 10.3, handbook of clay science. In: Bergaya, F., Theng, B.K.G., Lagaly, G. (Eds.), Developments in Clay Science, vol. 1. Elsevier, Amsterdam, pp. 583–621.

Sinha Ray, S., Okamoto, M., 2003. Polymer/layered silicate nanocomposites: a review from preparation to processing. Prog. Polym. Sci. 28, 1539–1641.

Vicente Rodríguez, M.A., Suárez Barrios, M., Bañares Muñoz, M.A., López González, J.D., 1996. Comparative FT-IR study of the removal of octahedral cations and structural modifications during acid treatment of several silicates. Spectrochim. Acta A 52, 1685–1694.

Wu, B., Qi, Sh., Wang, X., 2010. Thermal behaviour of poly(vinyl chloride) treated with montmorillonite–silica–3-triethoxysilyl-1-propanamine (K–Si–MMT) nanocomposites. Polym. Test. 29, 717–722.

Xi, Y., Ding, Z., He, H., Frost, R.L., 2004. Structure of organoclays an X-ray diffraction and thermogravimetric analysis study. J. Colloid Interface Sci. 277, 116–120.